

# Molecular dynamics studies for the temperature dependence of the local arrangements and dynamical properties of sodium ions in a one-dimensional tunnel-like space of hollandite

Yuichi Michiue\* and Mamoru Watanabe

Advanced Materials Laboratory, National Institute for Materials Science, 1-1 Namiki, Tsukuba, Ibaraki, 305-0044, Japan. E-mail: michiue.yuichi@nims.go.jp

Received 18th April 2001, Accepted 3rd September 2001  
 First published as an Advance Article on the web 23rd October 2001

Molecular dynamics simulations have been performed to investigate the temperature dependence of static and dynamical properties of Na<sup>+</sup> ions in a one-dimensional tunnel of the hollandite structure. Structural data including the Na<sup>+</sup> ion distribution obtained from diffraction experiments were well reproduced at room temperature and 773 K. Microscopic pictures and Fourier transforms of the velocity autocorrelation function clarified the diversity in dynamical behavior of Na<sup>+</sup> ions in a range between 300 and 1273 K. The difference between Ti–Na and Cr–Na pair correlation functions, suggesting the tendency of Na<sup>+</sup> ions to be closer to Cr<sup>3+</sup> rather than Ti<sup>4+</sup> in the framework structure, was significant up to at least 1273 K. Correlation of ionic motions is so strong at high temperature as to cause the collective translation of Na<sup>+</sup> ions in a few tunnels at 773 K and above.

## Introduction

Much attention has been paid to the static and dynamic behaviour of ions or molecules in small spaces like zeolite cages, because those spaces provide unique phenomena as well as practical uses like catalysts, molecular sieves, and so on. Cavities are two or three dimensionally connected in most microporous materials. On the other hand, there is a well-known series of metal oxides with one-dimensional (1-D) tunnel structures consisting of coordination MO<sub>6</sub> (M: metal) octahedra (Fig. 1). Todorokite has the largest tunnel of (3 × 3) octahedral units<sup>1</sup> and is referred to as an octahedral molecular sieve because it shows chemical activities such as hydrocarbon uptake<sup>2</sup> and catalytic reactions.<sup>3</sup> Hollandite containing (2 × 2) tunnels<sup>4</sup> (Fig. 2) is stable and well characterized. Smaller

tunnels of (1 × 1) and (1 × 2) having electrochemical activities are attracting much attention.<sup>5</sup> Some other types of tunnels with (2 × 3),<sup>6</sup> (2 × 4),<sup>7</sup> and (2 × 5)<sup>8</sup> have also been reported but are far from well-characterized because of their instability. The hollandite tunnel consists of a sequence of cavities available for accommodation of guest ions. Therefore, hollandite-like compounds are regarded as host materials with guest ions in a moderately small space, although the compounds are essentially different from the usual microporous materials in certain aspects. The small pore size of a hollandite tunnel results in the lack of chemical activity as a molecular sieve. Instead, hollandite-like compounds have been studied to utilize

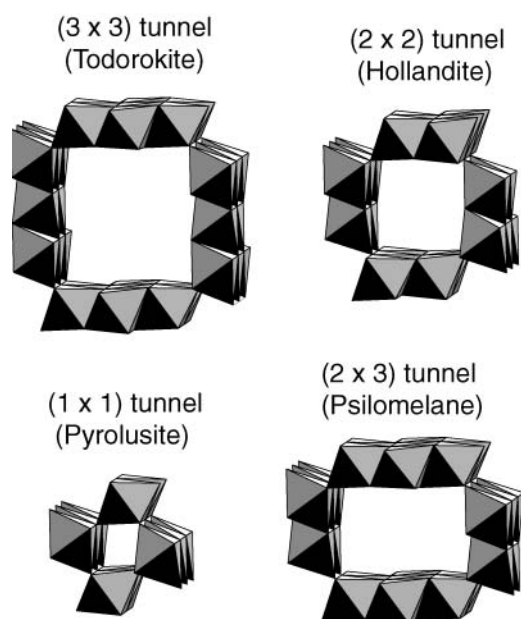


Fig. 1 Schematic representation of one-dimensional tunnel structures consisting of coordination octahedra.

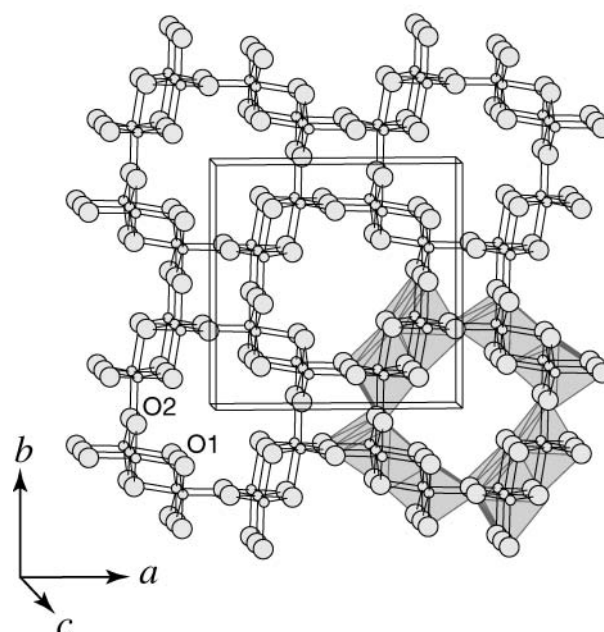
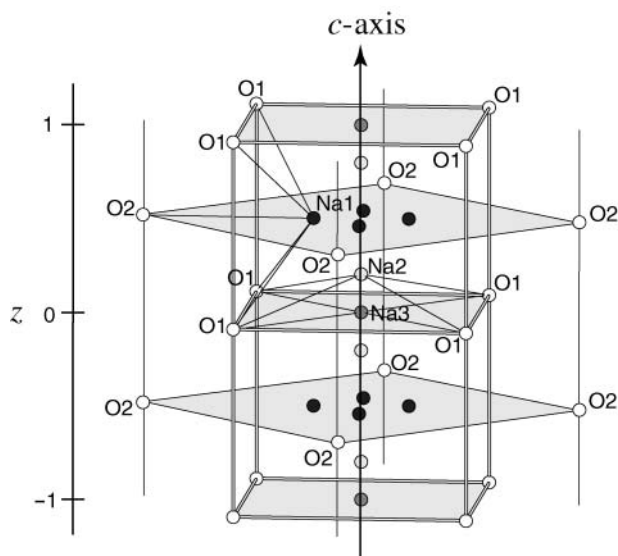


Fig. 2 A framework structure of hollandite forming (2 × 2) tunnels. Small circles are framework metal ions (Ti<sup>4+</sup> or Cr<sup>3+</sup>), and large circles are oxygen ions. Two kinds of crystallographically nonequivalent oxygen ions, O1 and O2, are seen. A part of the structure is drawn by a linkage of MO<sub>6</sub> coordination octahedra (shaded).



**Fig. 3** Schematic representation of oxygen-squares constructing the hollandite tunnel and possible Na<sup>+</sup> ion sites determined from the X-ray diffraction study.

the 1-D tunnel as (i) a host for immobilization of radioactive wastes<sup>9</sup> and (ii) a pathway for conduction of alkali ions.<sup>10,11</sup> In addition, one of the important characteristics of this material is the disordering of guest cations in a rigid framework structure. Distribution and dynamics of guest cations are complicated because each guest cation interacts with the framework structure and the other guest ions as well.<sup>12,13</sup> It is well known that sorbate–cation interactions are so strong in some zeolites as to cause displacement of cation locations,<sup>14,15</sup> while cation–cation interactions are prominent in hollandite structures for two reasons.<sup>12</sup> The first is low dimensionality of the space, and the second is a high density of guest cations; the cation content per cavity is about 75% or more and the distance between adjacent cavity centers is only about 3 Å.

We have been focusing on titanium based hollandite Na<sub>x</sub>Cr<sub>x</sub>Ti<sub>8-x</sub>O<sub>16</sub> ( $x \approx 1.7$ ) originally reported by Bayer *et al.*<sup>16</sup> The hollandite tunnel is constructed by the alternate stacking of two kinds of oxygen squares along the *c*-axis (Fig. 3). The smaller square is made up of four O1 oxygen ions (O1-square) and the larger one is of four O2 ions (O2-square). The tunnel wall consists of O1 ions forming a connection of pseudocubic cavities as shown in Fig. 3. The cavity is, however, usually described as a pseudocuboctahedron by including the second-nearest four O2 oxygen ions surrounding the O1-cube. If the cavities are fully occupied by guest cation, the chemical composition is Na<sub>2</sub>Cr<sub>2</sub>Ti<sub>6</sub>O<sub>16</sub>. Namely, the cation concentration for Na<sub>x</sub>Cr<sub>x</sub>Ti<sub>8-x</sub>O<sub>16</sub> is defined by  $x/2$ . The O1-square generally plays a role of bottleneck for transportation of large alkali cations such as K<sup>+</sup> and Rb<sup>+</sup> because the diagonal O1–O1 distance, about 5.2 Å in titanium based hollandites, is smaller than the sum of ionic sizes of O<sup>2-</sup> (2.8 Å) and K<sup>+</sup> (3.02 Å).<sup>17</sup> The center of the O1-square is, therefore, referred to as a bottleneck position. In the Na-salt, the size effect of the guest ion is clearly observed and the distribution of Na<sup>+</sup> ions with an ionic size of 2.32 Å is essentially different from those of K<sup>+</sup> and Rb<sup>+</sup>. X-Ray diffraction studies at room temperature have revealed that Na<sup>+</sup> ions are found at the bottleneck position (Na3 site in Fig. 3) as well as in a cuboctahedral cavity (Na1 and Na2 sites).<sup>18</sup> The Na1 site is deviated from the cavity center in one of the four directions normal to the tunnel axis (*c*-axis), which implies that the cavity is too large for a Na<sup>+</sup> ion to be stabilized at the center. The Na1 site has an interaction with one of the O2 ions 2.66 Å away and with 4 O1 ions (2.54 Å for two Na–O1 bonds and 2.60 Å for the remaining two Na–O1) as shown in Fig. 3. The Na2 site is shifted from the

cavity center along the tunnel axis and forms a rather uncommon square-pyramidal coordination with 4 O1 ions (Na2–O1: 2.63 Å). The Na3 site has a square-plane coordination of 4 O1 ions at a distance 2.57 Å which is a common value for that between Na<sup>+</sup> and O<sup>2-</sup> ions. These Na positions are roughly unchanged up to at least 773 K.<sup>19</sup> Such structural data based on X-ray diffraction experiments result from averaging of all the Na<sup>+</sup> ions in a whole crystal over a certain period of time far longer than that of thermal motion of ions. Local arrangements and dynamics of Na<sup>+</sup> ions in the tunnel are still ambiguous, while atomistic simulation by the molecular dynamics (MD) method provides us with microscopic pictures unavailable by conventional experiments.

It is important to clarify the properties of guest ions in microporous materials over a wide range of temperature, because the materials are practically used at elevated temperatures in most cases. However, MD studies of microporous materials at high temperatures are rare. This is partly because experimental data of the guest ion distribution, which is the most basic data for checking the validity of the simulation results, is unavailable for most microporous materials at high temperatures. In this paper we demonstrate that MD simulation using classical pairwise potentials can be a powerful tool to investigate the static and dynamic behaviour of guest cations over a wide range of temperature. Here we give some improvements and extensions of the preliminary study for the same material at 300 K:<sup>20</sup> (i) instead of the scaling method, Nose<sup>21</sup> and Andersen<sup>22</sup> methods are adopted to control temperature and pressure, respectively, (ii) calculation steps for both aging and analysis are increased to provide enough data to obtain correlation functions, and (iii) temperature is varied between 300 K and 1273 K. Structural aspects previously reported by X-ray diffraction experiments at room temperature and 773 K are compared with the simulation results. Furthermore, local structures and dynamical aspects of Na<sup>+</sup> ions are discussed on the basis of microscopic pictures and correlation functions.

## Method of calculation

The interionic potential used in the present study consists of three terms, a Coulomb interaction, a Gilbert-type repulsion,<sup>23</sup> and a dispersive interaction:

$$V_{ij}(r_{ij}) = z_i z_j e^2 / r_{ij} + f_0 (b_i + b_j) \exp[(a_i + a_j - r_{ij}) / (b_i + b_j)] - c_i c_j / r_{ij}^6$$

where  $z_i$  is the formal charge of the *i*th ion,  $e$  is the unit charge,  $r_{ij}$  is the distance between the *i*th and *j*th ions,  $f_0$  is the constant (1 kcal mol<sup>-1</sup> Å<sup>-1</sup>) and  $a_i$ ,  $b_i$  and  $c_i$  are related to size, softness and polarizability of the ion. Parameters are empirically determined to reproduce structures of many oxides.<sup>24</sup> Modifications were made as mentioned in the previous paper,<sup>20</sup> although the size parameter of Na was again changed a little so that the simulated occupation ratios at the three Na sites are closer to those from experiments at 300 K and 773 K. All parameters used are listed in Table 1.

The body-centered tetragonal unit cell of the hollandite structure has a space group *I4/m* and experimental cell dimensions  $a = b = 10.058$  Å and  $c = 2.957$  Å at room temperature. The extended cell consisting of 28 ( $= 2a \times 2b \times 7c$ ) unit cells was used for MD calculations. This cell contains 224

**Table 1** Parameters used for the calculation

	$z_i$	$a_i/\text{Å}$	$b_i/\text{Å}$	$c_i/\text{kcal}^{1/2} \text{mol}^{-1/2} \text{Å}^3$
Na	1.0	1.453	0.080	—
Ti	4.0	1.235	0.080	—
Cr	3.0	1.150	0.080	—
O	-2.0	1.629	0.085	20.0

framework metals (Ti or Cr) and 448 oxygen ions to form eight tunnels extending along the  $c$ -axis. Initial positions of the framework metals and oxygen ions were taken from the results of the X-ray diffraction study.<sup>18</sup> As no orderings of metal ions were detected from diffraction experiments, 48 sites for Cr were randomly selected among 224 framework metal positions and the rest are Ti. Note that there is no need to consider any site preference among Ti and Cr because all of the framework metal sites are crystallographically equivalent. Among 7 cavity centers in each tunnel, 6 are randomly chosen for location of  $\text{Na}^+$  ions, and one is kept empty. The chemical composition of this MD cell  $\text{Na}_{48/28}\text{Cr}_{48/28}\text{Ti}_{176/28}\text{O}_{448/28}$  approximates to the composition of crystals synthesized,  $\text{Na}_{1.7}\text{Cr}_{1.7}\text{Ti}_{6.3}\text{O}_{16}$ .

The calculation of 10000 steps after an initial aging of 10000 steps with an integration time of  $1.0 \times 10^{-15}$  s was performed by using the program MXDTRICL.<sup>25</sup> Pressure was set to the atmospheric pressure by the Andersen method<sup>22</sup> and temperature (300–1273 K) was controlled by the method proposed by Nose<sup>21</sup> (NPT-ensemble).

## Results and discussion

### Comparison with X-ray diffraction studies

The framework structure from the simulation is essentially identical to that determined by the X-ray study. The temperature dependence of cell parameters is given in Fig. 4 along with the data from X-ray diffraction experiments at 300 and 773 K. Deviations of the simulated cell parameters from experimental values were less than 2.5% at both of the temperatures. Each  $\text{Na}^+$  ion located at a cavity center moved off the initial position in the early stages of the aging process, because the cavity center is unsuitable for accommodation of a  $\text{Na}^+$  ion, as experimentally observed. In order to compare the results of the simulation with the average structure from X-ray analysis, distribution maps of  $\text{Na}^+$  ions were drawn from trajectories recorded at every 10 steps during simulations. The center axes of eight tunnels are  $(0, 0, z)$ ,  $(1, 0, z)$ ,  $(0, 1, z)$ ,  $(1, 1, z)$ ,  $(1/2, 1/2, z)$ ,  $(3/2, 1/2, z)$ ,  $(1/2, 3/2, z)$ , and  $(3/2, 3/2, z)$  in the MD cell of  $2a \times 2b$ . The first four tunnels have bottlenecks at  $z = n$  ( $n = 0, 1, \dots, 6$ ), while in the last four tunnels the bottleneck positions are at  $z = n + 1/2$  because of the body-centered unit cell. By considering the above relations between tunnels, all trajectories of  $\text{Na}^+$  ions are translated to equivalent positions in one cavity with the center  $(0, 0, 1/2)$ . Then,  $\text{Na}^+$  ions found

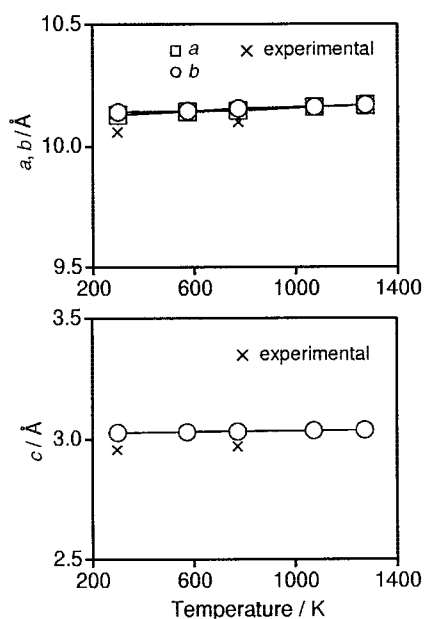


Fig. 4 Temperature dependence of cell parameters.

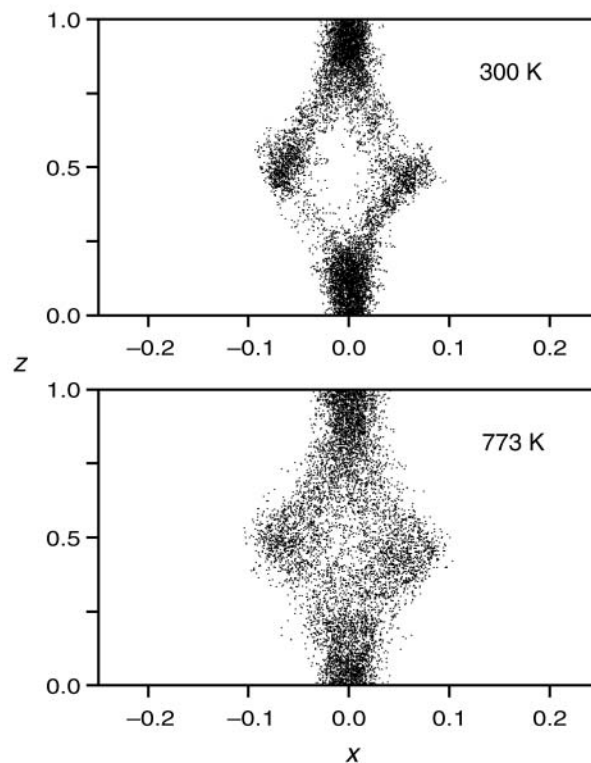
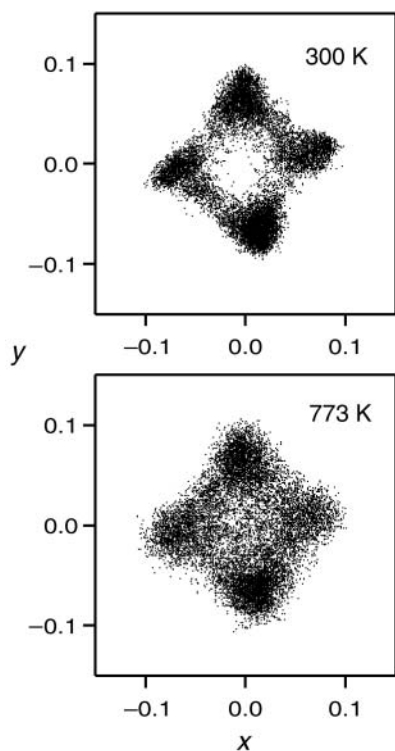


Fig. 5 Average distribution maps of  $\text{Na}^+$  ions parallel to the tunnel axis ( $-0.05 < y < 0.05$ ) from MD simulations at 300 K and 773 K.

in the range  $-0.05 < y < 0.05$  were plotted to give distribution maps at the plane parallel to the tunnel axis ( $c$ -axis) at 300 K and 773 K (Fig. 5). In ranges of  $0.25 > z$  and  $z > 0.75$ ,  $\text{Na}^+$  ions are close to the axis center of the tunnel, while a considerable number of  $\text{Na}^+$  ions have deviated from the axis center in the vicinity of  $z = 0.5$ . These features are in good agreement with the electron density obtained from X-ray diffraction data using the maximum-entropy method.<sup>26</sup> The former corresponds to the distribution at Na3  $(0, 0, 0)$  and Na2  $(0, 0, \pm 0.203)$  sites. The latter reflects the distribution at the Na1 site, because these  $\text{Na}^+$  ions are concentrated at positions close to those determined by X-ray diffraction studies at room temperature,  $(0.072, 0.014, 0.5)$  and crystallographically equivalent positions  $(-0.014, 0.072, 0.5)$ ,  $(-0.072, -0.014, 0.5)$ ,  $(0.014, -0.072, 0.5)$ . Splitting of the distribution into four positions is clearly seen in Fig. 6 where  $\text{Na}^+$  ions in the range  $0.45 < z < 0.55$  are plotted. With increasing temperature, the distribution naturally became broader, but the  $\text{Na}^+$  positions were little changed, as experimentally observed; Na1:  $(0.071, 0.010, 0.5)$ , Na2:  $(0, 0, 0.24)$ , and Na3:  $(0, 0, 0)$  at 773 K.<sup>19</sup>

For a more quantitative discussion Na contents at the Na sites were calculated from the trajectories of the ions.  $\text{Na}^+$  ions within  $1.0 \text{ \AA}$  of a site (*i.e.* Na1, Na2, or Na3 site) at a certain step were considered to occupy the site at that instance. If two or more sites satisfied this criterion for one  $\text{Na}^+$  ion, the ion was assigned to the nearest site. By assignment of the trajectories of all  $\text{Na}^+$  ions, 52% were allotted to the Na1 site, 30% were for the Na2, and the rest, 18%, were at the Na3 site at 300 K. On the other hand, occupation ratios at these sites reported from the X-ray diffraction experiment at 295 K are 0.11 at the Na1, 0.16 at the Na2, and 0.10 at the Na3 site.<sup>18</sup> As four Na1, two Na2 and one Na3 sites are in a cavity,  $0.44 (= 0.11 \times 4)$  is allotted for the Na content at the Na1 site in a cavity,  $0.32 (= 0.16 \times 2)$  for the Na2 site, and 0.10 for the Na3 site. The ratios, as a percentage, are 51% for the Na1 site, 37% for the Na2, and 12% for the Na3. Occupational parameters at the Na2 and Na3 sites obtained from X-ray diffraction data are strongly correlated to each other because the two sites are very



**Fig. 6** Deviation of  $\text{Na}^+$  ions from the cavity center at the plane normal to the tunnel axis ( $0.45 < z < 0.55$ ) from MD simulations at 300 K and 773 K.

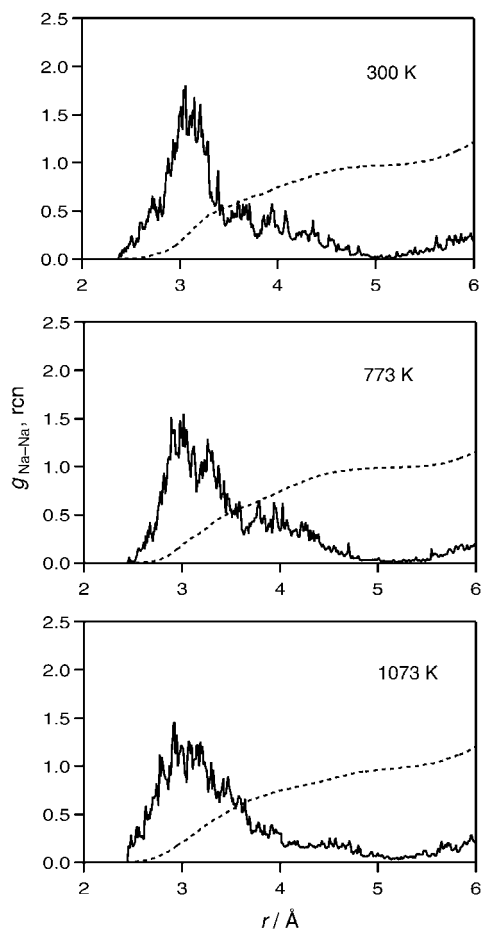


**Fig. 7** Na–Na pair correlation functions (solid line) and running coordination number (dotted line) at 300, 773, and 1073 K.

close. It is, therefore, more adequate to deal with the sum of the ions at the Na2 and the Na3 sites, rather than to discuss the two sites separately. The ratio of Na1 : (Na2 + Na3) = 52 : 48 from the simulation is very close to that from the experiment, 51 : 49. The ratios similarly estimated at 773 K are 53% for the Na1 site and 47% for (Na2 + Na3) from the simulation, and 56% for the Na1 and 44% for (Na2 + Na3) from the experiment. Thus the simulation results are in good agreement with those from diffraction experiments at 300 K and 773 K.

### Local arrangements and dynamical properties

The Na–Na pair correlation function  $g_{\text{Na-Na}}(r)$  and running coordination number  $\text{rcn}(r)$  are shown in Fig. 7, where no contribution from inter-tunnel Na–Na pairs, that is between ions in different tunnels, is included because the distance from a tunnel to the nearest one exceeds 7 Å. It is generally expected that  $\text{Na}^+$  ions in a smooth tunnel are arranged with similar intervals around  $clp \approx 3/0.85 \approx 3.5$  Å ( $c$ :  $c$ -axis dimension,  $p$ : concentration of  $\text{Na}^+$  ions per unit cell) so as to reduce repulsive interactions between themselves. However,  $g_{\text{Na-Na}}(r)$  shows a broad distribution between 2.4 and 5.1 Å, which primarily reflects the fact that  $\text{Na}^+$  ions are forced to locate around certain positions in a tunnel under the influence of the framework potential. Thus, an arrangement of guest ions is complicated by the coexistence of two competing effects, host–guest and guest–guest interactions. The interatomic distances between Na positions obtained from X-ray diffraction experiments are given in Fig. 8. It is obviously impossible for  $\text{Na}^+$  ions to occupy some of these sites at the same time because the neighboring positions such as  $\text{Na1}^i\text{--Na2}^{ii}$  and  $\text{Na2}^i\text{--Na3}^i$  are too close. Judging from Fig. 7 and 8, 11 types of Na–Na pairs with an interatomic distance between 2.4 and 5.1 Å are possible;  $\text{Na1}^i\text{--Na1}^{iv}$ ,  $\text{Na1}^i\text{--Na1}^v$ ,  $\text{Na1}^i\text{--Na2}^{iv}$ ,  $\text{Na1}^i\text{--Na2}^v$ ,

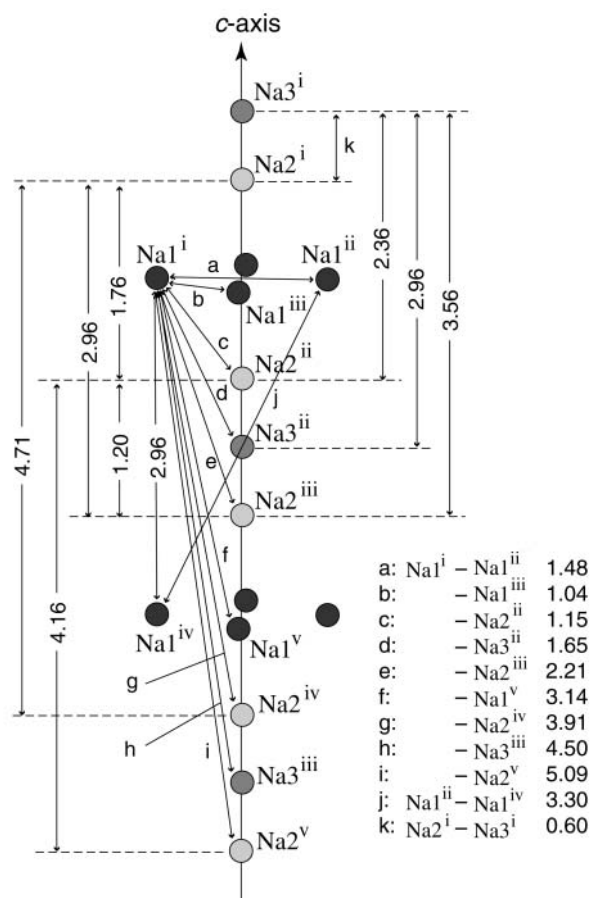


**Fig. 8** Possible Na–Na distances (Å) less than 5.1 Å. Na positions drawn are from X-ray diffraction data. Crystallographically equivalent positions are discriminated by superscripts.

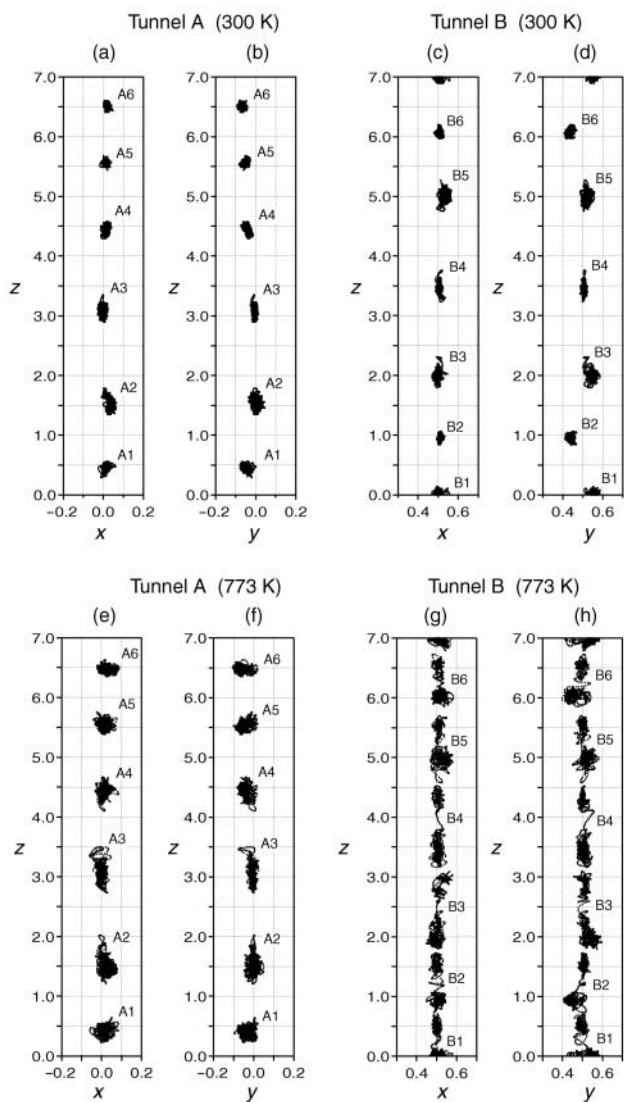


**Fig. 9** Trajectories of  $\text{Na}^+$  ions in two selected tunnels at 300 K and 773 K.

$\text{Na1}^i\text{-Na3}^{iii}$ ,  $\text{Na1}^{ii}\text{-Na1}^{iv}$ ,  $\text{Na2}^i\text{-Na2}^{iii}$ ,  $\text{Na2}^i\text{-Na2}^{iv}$ ,  $\text{Na2}^{ii}\text{-Na2}^v$ ,  $\text{Na2}^{iii}\text{-Na3}^i$ , and  $\text{Na3}^i\text{-Na3}^{ii}$ . To confirm this from microscopic pictures, trajectories of  $\text{Na}^+$  ions in two of the eight tunnels are plotted (Fig. 9). Bottleneck positions are at  $z=n$  ( $n=0, 1, 2, \dots, 6$ ) for the tunnel A extending around the center axis (0, 0,  $z$ ), while at  $z=n+1/2$  for the tunnel B extending around (1/2, 1/2,  $z$ ). A5 and A6 ions are assigned as  $\text{Na}^+$  ions located at the Na1 site, (−0.01, 0.07, 5.5) and (−0.01, 0.07, 6.5), respectively. A2 moves between the Na1 (0.07, 0.01, 1.5) and the Na2 (0, 0, 1.8) site. A1 and A4 ions show similar behavior to A2. A3 is between the Na2 (0, 0, 3.2) and the Na3 (0, 0, 3) site.  $\text{Na}^+$  ions migrating between crystallographically nonequivalent positions even at room temperature are commonly observed in zeolite structures.<sup>27–29</sup> When A2 is at a Na2 site and A3 is at a Na3 site, the interatomic distance is roughly estimated to be 3.56 Å, because the relation of the two ions is the same to that of  $\text{Na2}^{iii}$  and  $\text{Na3}^i$  in Fig. 8. Three Na–Na pairs,  $\text{Na1}^i\text{-Na2}^v$ ,  $\text{Na1}^i\text{-Na3}^{iii}$ , and  $\text{Na2}^{ii}\text{-Na2}^v$  are also possible for A2 and A3. Thus, by examining for all of the ion-pairs in tunnel A at 300 K, such as A1–A2, A3–A4, ..., A6–A1, 9 of 11 types of the Na–Na pairs listed above are actually found. One of the probable snapshots of  $\text{Na}^+$  ions in the tunnel is schematically shown in Fig. 10. This figure suggests that the Na2 site is necessary to make  $\text{Na}^+$  ions arrange at roughly uniform intervals, reducing repulsive interactions between them. This could be an explanation for the fact that some  $\text{Na}^+$  ions are found at the Na2 site forming the uncommon  $\text{NaO}_4$

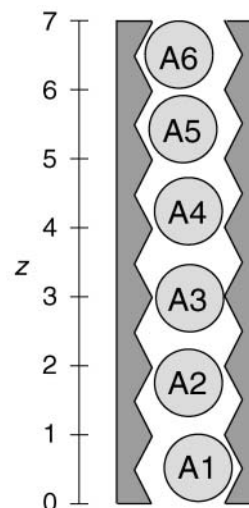


**Fig. 10** Schematic representation for one of the probable snapshots of  $\text{Na}^+$  ions in a tunnel.

square-pyramidal coordination despite the nearby square-plane coordination site, Na3, which is suitable for accommodation of a  $\text{Na}^+$  ion. These features are essentially identical to those in tunnel B and highly probable for the actual behavior of ions confined in a one-dimensional space in high density.

The arrangement of  $\text{Na}^+$  ions in tunnel A is similar even at 773 K, while thoroughly disturbed in tunnel B.  $\text{Na}^+$  ions in tunnel B fluctuate along the  $c$ -axis at 773 K (Fig. 11(a)), which

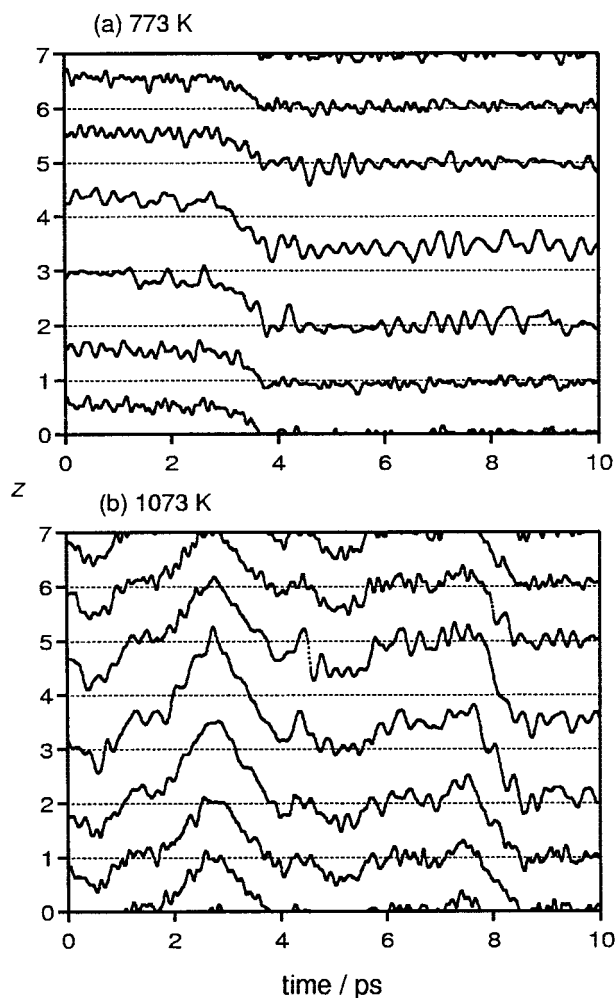


**Fig. 11** Fluctuation of  $z$  coordinates for  $\text{Na}^+$  ions in a tunnel. (a) 773 K, (b) 1073 K.

clearly explains the continuous distribution of the  $\text{Na}^+$  plot in Fig. 9(g) and 9(h). This phenomenon, characterized as a kind of collective translation, is a unique aspect of the behavior of guest ions in a confined space. Similar behavior of Na ions was also seen in the simulation of zeolites.<sup>30</sup> In the hollandite structure, the low dimensionality of the space and the high density of the guest ions may be responsible for a strong correlation between  $\text{Na}^+$  ions which is enhanced with increasing temperature (Fig. 11(b)). The situation can be regarded as the coexistence of a solid (the framework structure) and fluids (guest ions). Similar behavior was observed in one more tunnel amongst the eight tunnels in the MD cell, while the rest are like tunnel A, even at 1273 K. Adjacent Na–Na distances were kept roughly constant when the collective translation occurred, which results in  $g_{\text{Na-Na}}(r)$  and  $\text{rcn}(r)$  at 773 and 1073 K being similar to those at 300 K. It should be noted that the microscopic behavior of  $\text{Na}^+$  ions at 1073 K (Fig. 11(b)) is quite different from that at 300 K despite no drastic change in the  $g_{\text{Na-Na}}(r)$  functions.

Fourier transforms of the velocity autocorrelation function along the tunnel axis ( $c$ -axis) for  $\text{Na}^+$  ions are shown in Fig. 12. Power spectra are obtained by averaging for all  $\text{Na}^+$  ions, while Fig. 9 suggests that the dynamical behavior of the  $\text{Na}^+$  ions are different from each other. Actually, the spectra calculated for each  $\text{Na}^+$  ion in tunnel A show considerable diversity. For example, the spectrum for the A3 ion (Fig. 13) has only the lower frequency components, while the A5 ion contains the higher frequency components. It seems that the A5 ion is tightly trapped at one of the NaI sites, as is supported by Fig. 9. This trapping might be concerned with the fact that framework-metal sites close to this position are occupied by  $\text{Cr}^{3+}$  ions by chance, as schematically shown in Fig. 14. This is naturally acceptable because the positive charge of  $\text{Cr}^{3+}$  is smaller than that of  $\text{Ti}^{4+}$ . An overall estimation for the effect of Cr-substitution on attracting  $\text{Na}^+$  ions can be obtained by comparing the pair correlation functions  $g_{\text{Cr-Na}}(r)$  and  $g_{\text{Ti-Na}}(r)$  (Fig. 15). The  $g_{\text{Cr-Na}}(r)$  gives higher values than  $g_{\text{Ti-Na}}(r)$  in the range  $r < 3.8 \text{ \AA}$ . This means that  $\text{Na}^+$  ions, as a whole, tend to be closer to  $\text{CrO}_6$  octahedra than  $\text{TiO}_6$ . The

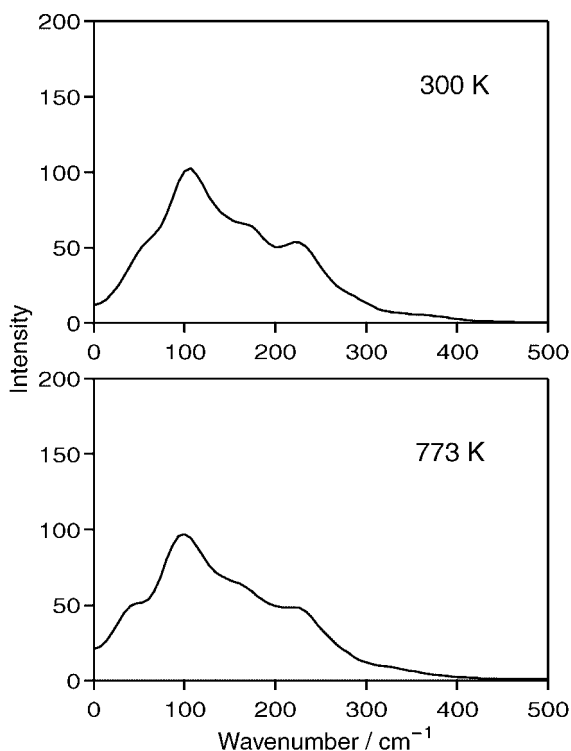


Fig. 12 Fourier transforms of velocity autocorrelation functions along the  $c$ -axis.

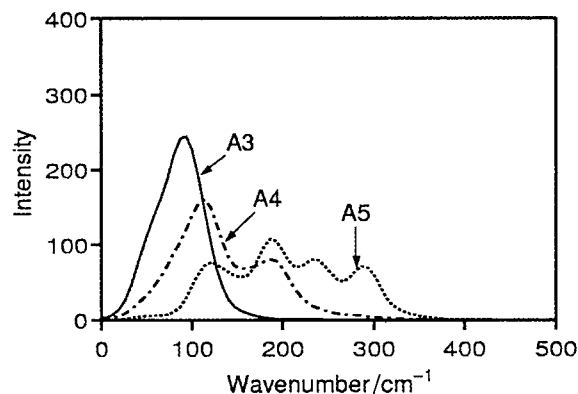


Fig. 13 Fourier transforms of velocity autocorrelation functions calculated for the individual  $\text{Na}^+$  ion.

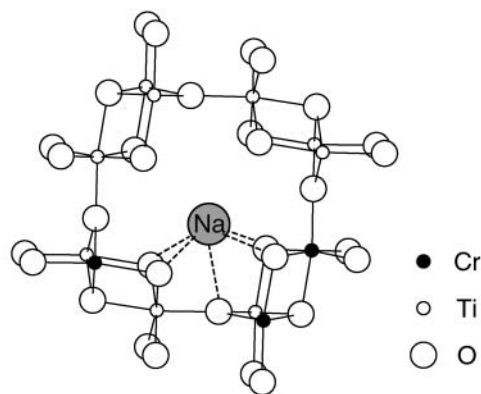


Fig. 14 Schematic representation of the  $\text{Na}^+$  ion shift toward  $\text{Cr}^{3+}$  ions.

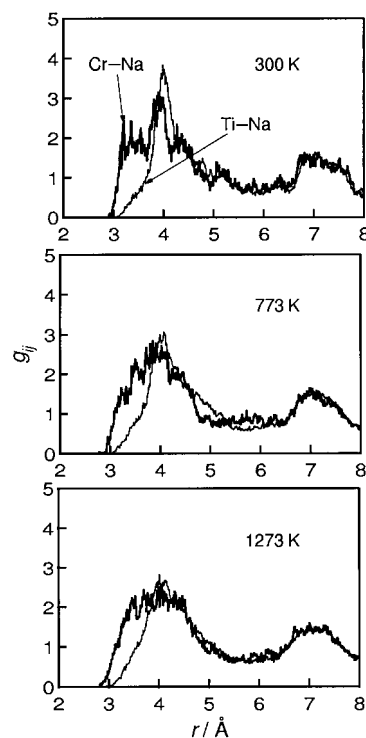


Fig. 15 Comparison between Ti–Na (thin line) and Cr–Na (thick line) pair correlation functions at 300, 773, and 1273 K.

difference between the two functions decreases with increasing temperature, but is still significant at 1273 K. Although the present simulation is based on classical pair potentials, the

results are conceivable because similar effects of Al<sup>3+</sup> substitution for Si<sup>4+</sup> on cation location are seen in zeolites by density functional studies.<sup>31</sup> Strong correlations between framework aluminium siting and guest cation distribution are also reported in heulandite-type zeolites having a two-dimensional channel system.<sup>32</sup> Different features in powder spectra between Na<sup>+</sup> ions in tunnel A are kept even at 1273 K. On the other hand, all Na<sup>+</sup> ions in tunnel B have similar dynamical properties at 1073 K and above, because these ions change their environment in accordance with collective translation as seen in Fig. 11.

## Conclusions

Local arrangements and dynamical properties of Na<sup>+</sup> ions in a one-dimensional tunnel of hollandite were studied by the molecular dynamics method over a temperature range of 300–1273 K. The characteristic distribution of Na<sup>+</sup> ions in the tunnel, as determined experimentally, was reproduced by the simulations qualitatively and quantitatively at 773 K as well as at room temperature. Na<sup>+</sup> ion trajectories showed that ions partially occupy the three kinds of positions determined from X-ray diffraction studies, keeping enough distance from neighboring ions to reduce repulsive interactions, which resulted in a broad distribution of the Na–Na pair correlation function over a range of 2.4–5.1 Å. Microscopic pictures and Fourier transforms of the velocity autocorrelation function have shown diversity in dynamical properties of Na<sup>+</sup> ions. Some of the Na<sup>+</sup> ions were tightly trapped at certain positions, while others fluctuated between neighboring Na sites even at room temperature. On the other hand, correlations in ionic motions are so strong that the collective translation of Na<sup>+</sup> ions was observed in a few tunnels at 773 K and above, which is a unique aspect for the behavior of guest ions in a confined space. It was suggested that the Cr-substitution for Ti at framework-metal sites can be a factor for preventing such a translation. The pair correlation function between Cr–Na gave higher values than those of Ti–Na in a range  $r < 3.8$  Å over the temperature range examined. This implies that Na<sup>+</sup> ions have a tendency to be closer to Cr<sup>3+</sup> ions in the framework structure and are trapped there even at high temperatures.

## References

- 1 S. Turner and P. R. Buseck, *Science*, 1981, **212**, 1024.
- 2 Y. F. Shen, R. P. Zenger, R. N. DeGuzman, S. L. Suib, L. McCurdy, D. I. Potter and C. L. O'Young, *Science*, 1993, **260**, 511.
- 3 Y. F. Shen, S. L. Suib and C. L. O'Young, *J. Am. Chem. Soc.*, 1994, **116**, 11020.
- 4 A. Bystrom and A. M. Bystrom, *Acta Crystallogr.*, 1950, **3**, 146.
- 5 S. Turner and P. R. Buseck, *Nature*, 1983, **304**, 143.
- 6 S. Turner and P. R. Buseck, *Science*, 1979, **203**, 456.
- 7 T. Riziha, H. Gies and J. Rius, *Eur. J. Mineral.*, 1996, **8**, 675.
- 8 O. Tamada and N. Yamamoto, *Mineral. J.*, 1986, **13**, 130.
- 9 A. E. Ringwood, S. E. Kesson, N. G. Ware, W. Hibberson and A. Major, *Nature*, 1979, **278**, 219.
- 10 J. Bernasconi, H. U. Beyeler and S. Strassler, *Phys. Rev. Lett.*, 1979, **42**, 819.
- 11 S. Yoshikado, T. Ohachi, I. Taniguchi, Y. Onoda, M. Watanabe and Y. Fujiki, *Solid State Ionics*, 1983, **9**, 1305.
- 12 H. U. Beyeler, *Phys. Rev. Lett.*, 1976, **37**, 1557.
- 13 H. P. Weber and H. Schulz, *J. Chem. Phys.*, 1986, **85**, 475.
- 14 C. P. Grey, F. I. Poshni, F. Gualtieri, P. Norby, J. C. Hanson and D. R. Corbin, *J. Am. Chem. Soc.*, 1997, **119**, 1981.
- 15 G. Vitale, C. F. Mellot, L. M. Bull and A. K. Cheetham, *J. Phys. Chem. B*, 1997, **101**, 4559.
- 16 G. Bayer and W. Hoffmann, *Z. Kristallogr.*, 1965, **121**, 9.
- 17 R. D. Shannon, *Acta Crystallogr., Sect. A*, 1976, **32**, 751.
- 18 Y. Michiue and M. Watanabe, *J. Solid State Chem.*, 1995, **116**, 296.
- 19 Y. Michiue, S. Yoshikado and M. Watanabe, *Solid State Ionics*, 2000, **136**, 939.
- 20 Y. Michiue and M. Watanabe, *J. Phys. Chem. Solids*, 1996, **57**, 547.
- 21 S. Nose, *J. Chem. Phys.*, 1984, **81**, 511.
- 22 H. C. Andersen, *J. Chem. Phys.*, 1980, **72**, 2384.
- 23 T. L. Gilbert, *J. Chem. Phys.*, 1968, **49**, 2640.
- 24 K. Kawamura, in *Molecular Dynamics Simulations*, ed. F. Yonezawa, Springer-Verlag, Berlin, 1992, p. 88.
- 25 K. Kawamura, computer code MXDTRICL, JCPE (Japan Chemical Program Exchange), Tokyo, 1996.
- 26 Y. Michiue and M. Watanabe, *Solid State Ionics*, 1995, **79**, 116.
- 27 J. M. Shin, K. T. No and M. S. Jhon, *J. Phys. Chem.*, 1988, **92**, 4533.
- 28 S. H. Lee, G. K. Moon, S. G. Choi and H. S. Kim, *J. Phys. Chem.*, 1994, **98**, 1561.
- 29 D. A. Faux, *J. Phys. Chem. B*, 1998, **102**, 10658.
- 30 F. Jaramillo and S. M. Auerbach, *J. Phys. Chem. B*, 1999, **103**, 9589.
- 31 G. N. Vayssilov, M. Staufer, T. Belling, K. M. Neyman, H. Knozinger and N. Rosch, *J. Phys. Chem. B*, 1999, **103**, 7920.
- 32 Y. M. Channon, C. R. A. Catlow, R. A. Jackson and S. L. Owens, *Microporous Mesoporous Mater.*, 1998, **24**, 153.